Independent Components of Magnetoencephalography, Part II: Single-trial Response Onset Times

Akaysha C. Tang,[123*] **Barak A. Pearlmutter**,[23]
Dan B. Phung, **Natalie A. Malaszenko**

Departments of [1]Psychology, [2]Computer Science, [3]Neurosciences,
University of New Mexico, Albuquerque, NM 87131, USA

Draft of July 29, 2001

Abstract

In the companion paper, we demonstrated that second-order blind identification (SOBI), an independent component analysis (ICA) method, can separate the mixture of neuronal and noise signals in magnetoencephalographic (MEG) data into neuroanatomically and neurophysiologically meaningful components, and that under relatively poor signal-to-noise conditions, SOBI offers a particular advantage in identifying and localizing neuronal source activations that are otherwise difficult to localize. In this paper, we explored the utility of SOBI in the temporal domain. By applying a simple threshold-crossing method to SOBI-separated neuronal components, we measured single-trial response onset times of neuronal populations activated during both cognitive and simple sensory activation tasks. We showed that response onset times can be measured in single trials in visual, auditory, and somatosensory modalities, with a detection rate as high as 96% under optimal conditions. These results, along with the localization results described in the companion paper, demonstrated that it is possible to non-invasively measure human single trial response onset times with millisecond resolution for specific neuronal populations from multiple sensory modalities. This capability makes it possible to study a wide range of perceptual and memory functions that critically depend on the timing of discrete neuronal events.

1 Introduction

Many fundamental questions in neuroscience have to do with the precise timing of discrete neuronal events (Sejnowski, 1995; Rieke et al., 1996). In animal models, electrophysiological techniques permit the measurement of rapidly occurring electrical events on the order of milliseconds.

*Corresponding author: Dept of Psychology, Logan Hall, University of New Mexico, Albuquerque, NM 87131, 505 277-4025 (voice), 505 277-1394 (fax), akaysha@unm.edu.

These fine temporal details in non-averaged signals can encode sensory information (Abeles et al., 1993; deCharms and Merzenich, 1996) and are critical for neural plasticity (Huerta and Lisman, 1993; Markram et al., 1997) and memory consolidation (Wilson and McNaughton, 1994). In humans, although both electroencephalography (EEG) and magnetoencephalography (MEG) offer millisecond temporal resolution, the need for signal averaging has made it difficult to use these techniques to non-invasively measure the precise timing of neuronal population responses in single trials.

One difficulty in measuring single-trial response onset times in MEG arises from the relatively poor signal-to-noise ratio. To deal with this problem, typical MEG data analysis is performed on the stimulus- or response-triggered averages. Consequently, only averaged timing information is available. Recently, ICA methods have been demonstrated to be particularly helpful in separating noise signals from neuromagnetic signals and in separating neuromagnetic signals from different neuronal populations (Vigário et al., 1998, 1999; Tang et al., 1999, 2000). The effectiveness and high performance of the ICA in MEG data analysis has also been demonstrated in its application to single-trial phantom data (Cao et al., 2000). Here, we explored the ability of ICA to separate the mixture of neuromagnetic signals into sufficiently clean functional components to allow estimates of single-trial *response onset times* from MEG data collected during cognitive (low signal to noise) and sensory activation (high signal to noise) tasks.

Previously, by applying the second-order blind identification (SOBI) method (Belouchrani et al., 1993; Cardoso, 1994) to MEG data, we were able to clearly separate various noise sources from neuronal sources and to segregat visual sources from different processing stages from each other (Tang et al., 1999, 2000). In the companion paper, we demonstrated that the resulting separated neuronal sources can be localized to neuroanatomically and neurophysiologically meaningful locations with cross-subject and cross-task reproducibility and with increased detectability. In this paper we further demonstrate the potential for applying SOBI to MEG for measuring non-averaged, single-trial response latencies from visual, auditory, and somatosensory sources.

2 Methods

We applied SOBI to MEG data collected during four cognitive tasks (described in Part I) and during a simple sensory activation task (binaural 500 Hz tone, 200 ms, 3.25 ± 0.125 ms SOA). These tasks offer data collected under both poor and good signal to noise conditions (cognitive tasks: poor; sensory activation task: good) and data involving activation of neuronal sources from three major sensory modalities. Single-trial visual, somatosensory, and auditory response onset times were estimated from components identified using SOBI.

First, we briefly summarize the process of applying SOBI to MEG data. We then proceeded to describe the detailed procedure for measuring single-trial response onset times. (For details on SOBI, localization of SOBI separated components, and the behavioral tasks, see the Methods and Appendix of the companion paper.)

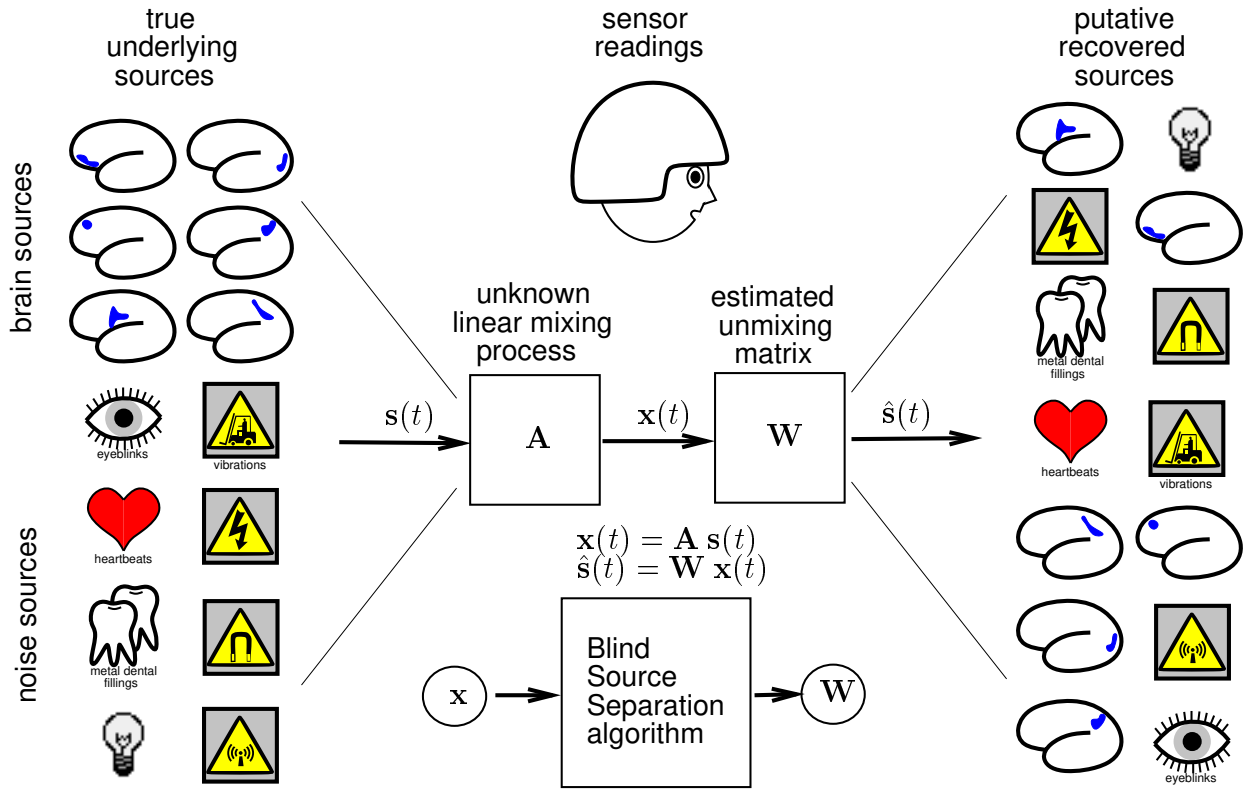

Figure 1: The ICA process. Signals from the brain and other noise sources $\mathbf{s}(t)$ are mixed through an unknown linear mixing process $\mathbf{A}$, resulting in the sensor readings $\mathbf{x}(t) = \mathbf{A}\mathbf{s}(t)$. ICA finds an unmixing matrix $\mathbf{W}$ that maps from the sensor signals to recovered components $\hat{\mathbf{s}}(t) = \mathbf{W}\mathbf{x}(t)$. The entries of the attenuation matrix $\mathbf{A} = \mathbf{W}^{-1}$ describe how strongly each sensor responds to each component.

2.1 Inputs and Outputs

The inputs to SOBI are time-varying vectors $\mathbf{x}(t)$ containing the continuous (*i.e.* not averaged) MEG time series from all 122 sensors for the entire period of the experiment, sampled at 300 Hz (cognitive tasks) and 600 Hz (auditory sensory activation) and bandpass filtered at 1–100 Hz. The output of the algorithm is a 122×122 matrix, $\mathbf{W}$, which maps from the vector of sensor values $\mathbf{x}(t)$ to the vector of recovered component values $\hat{\mathbf{s}}(t) = \mathbf{W}\ \mathbf{x}(t)$ (Fig. 1), up to a scaling and permutation of the components. Using the matrix $\mathbf{W}$, one maps the input sensor signals $\mathbf{x}(t)$ to the recovered component signals $\hat{\mathbf{s}}(t)$.

2.2 SOBI Components in Time

The recovered components $\hat{\mathbf{s}}_i(t)$ can be displayed as a plot of signal strength as a function of time, or alternatively in an *MEG image* (*e.g.* Fig. 2b), a pseudo-colored bitmap in which the responses of a given component during an entire experiment can be parsimoniously displayed (Jung et al., 1999). Typically, each row represents one discrete trial of stimulation and multiple trials are ordered vertically from top to bottom. MEG images will be used throughout this paper to provide temporal

information, such as the single-trial response onset times of a given separated component.

2.3 SOBI Components in Space

Although SOBI does not assume any physical model of the neuronal source generators, spatial information concerning a separated component is given by its field map, which represents the measured *sensor* response to the activation of the component $\hat{s}_i(t)$. The field map (*e.g.* Fig. 5b) of the i^{th} component $\hat{s}_i(t)$ is the i^{th} column of the estimated attenuation matrix $\hat{\mathbf{A}}$, where $\hat{\mathbf{A}} = \mathbf{W}^{-1}$. In combination with the structural MRI, the field maps can be used as input to standard tools for localizing the separated components within the brain (see Part I and *e.g.* Fig. 5c).

2.4 Identification of Neuronal Sources

Before estimating single-trial response onset times, neuronal sources were first identified by computing various event-triggered averages for each component, *e.g.* visual, auditory, or somatosensory stimulus-locked averages. If a component unambiguously shows an event-triggered response in the average and if the component can be localized to a meaningful location within the brain (for details, see companion paper), then this component is considered a neuronal source. Of all 122 components recovered, only a small portion showed event-locked responses. Although the exact number will depend on the task, typically less than 20 components showed evoked responses in these experiments.

2.5 Single-trial Response Onset Time Detection

Single-trial response onset time detection is performed only when there is an evoked response that clearly deviates from the baseline in the averaged component data. For all identified neuronal sources, we estimated response onset times by the leading edge of the response, rather than the time of the peak response. This measure is more robust against noise and also better captures the intuitive goal of detecting the time of the earliest detectable response, rather than of the maximal response.

The process of single-trial response onset detection is iterative: both the threshold and detection windows are adjusted until no further reduction in false detection can be achieved. An initial threshold was set between the peak amplitude and one-half of the peak amplitude in the event-triggered averages plot. The beginning of the detection window initially was set at the time the event-triggered averages first exceeded the range of baseline fluctuation. The detection window ended when the event-triggered averages first returned to the same level as when the detection window began.

Because single-trial responses can be very different from the event-triggered averages, the threshold and detection window were adjusted through an iterative process to ensure that no responses were excluded. Although some of the components showed biphasic responses, the single-trial response time analysis presented here focused solely on the initial phase of the response. Using the initial threshold and detection window, response onset times were determined and graphically superimposed on the MEG image (detected response time, or DRT, curve) to allow visual verification of the detected onset times.

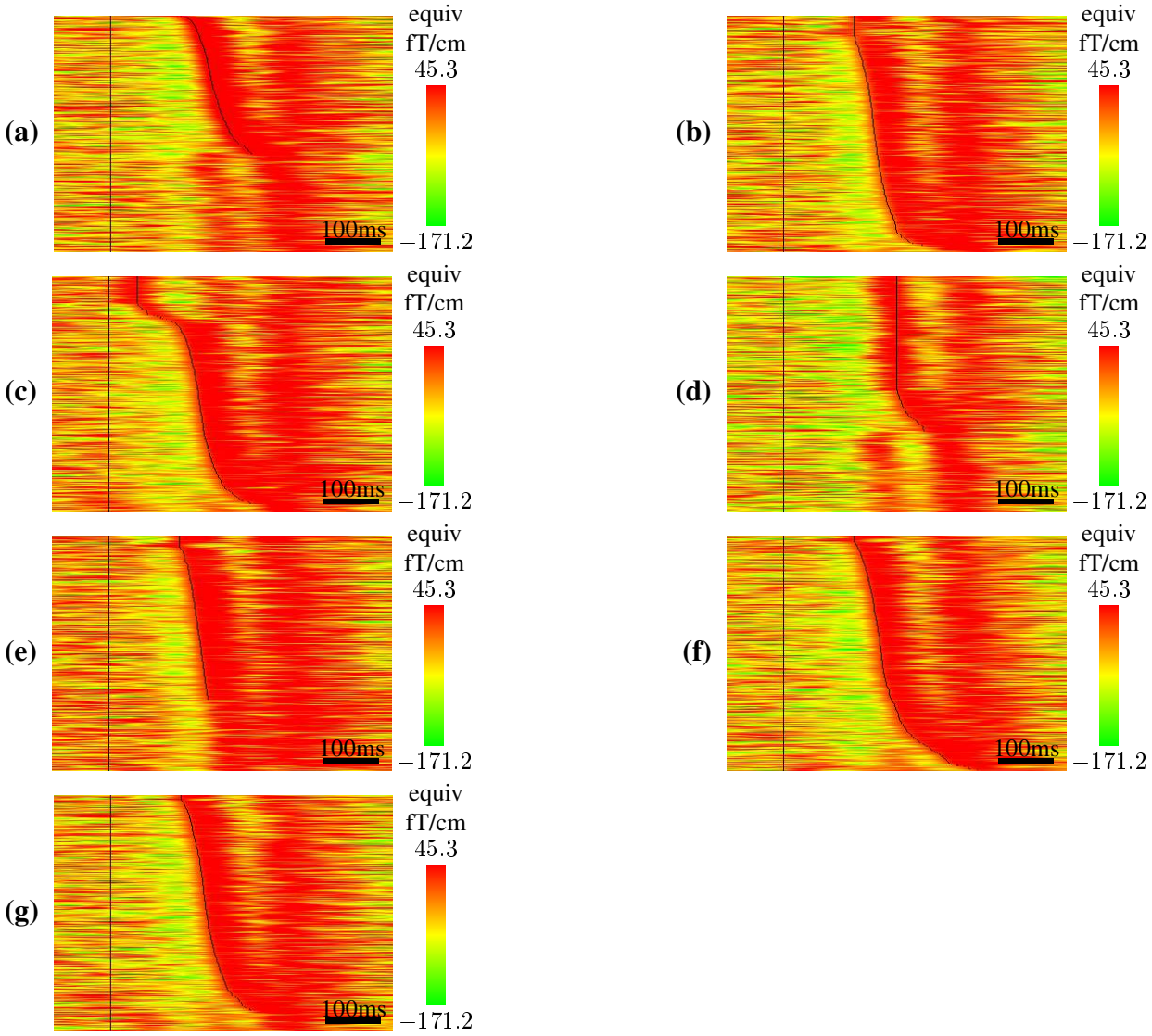

Figure 2: Examples of sub-optimal dection due to **(a)** too high a threshold; **(b)** too low a threshold; **(c)** too early a beginning window (w_b); **(d)** too late a beginning window (w_b); **(e)** too early an end window (w_e); **(f)** too late an end window (w_e); and **(g)** an optimal detection.

2.6 Threshold

If the threshold is set too high, one may overestimate the onset times by missing the initial onset times or leave many trials undetected. Overestimation of onset times is easily seen as a right shift in the DRT curve from the leading edge of color change associated with the responses (Fig. 2a). Because MEG images are generated in such a way that all trials with responses detected are displayed on top and sorted in increasing DRT and all trials with no responses detected are displayed at the bottom, missing responses are apparent under visual inspection as shown at the bottom of Fig. 2a. If the threshold is set too low, false detection can occur when the amplitude of baseline fluctuation is relatively large. In this case the DRT curve will show a clear discontinuity, with the point of discontinuity separating trials of false detection (sometimes a vertical line) from trials of

correct detection (smooth curve), as in Fig. 2b. In both cases, the threshold could be either lowered or raised accordingly in the next iteration.

2.7 Detection Window

Once the detection threshold is determined, one further examines the MEG image for false detections associated with incorrect settings of the beginning (w_b) and ending (w_e) of the detection window. If w_b is too early, the response window will include a part of the baseline and false detections similar to those caused by a low threshold (Fig. 2c). If w_b is too late, the DRT curve will begin with a vertical line, indicating a detected response at w_b (Fig. 2d). If w_e is too early, responses may be missing (see bottom portion of Fig. 2e). This case can be identified using a method similar to that for identifying missing trials due to too high a threshold. If w_e is too late, a late portion of a biphasic response will be falsely detected as the initial response. This form of false detection is easily seen near the tail end of the DRT curve (Fig. 2f) where initial responses were clearly missed, while the second phase of the responses were marked. In any of the above cases, one can adjust the detection window parameters for the next iteration.

For each neuronal source, this iterative process continues until no further reduction in the frequency of false detections or missing responses can be achieved. Statistics on the detected onset times are then computed and reported along with the resulting MEG image (Fig. 2g).

3 Results

3.1 Effect of Filter Length on Detected Onset Times

As filtering can affect response onset times, we first investigated the effect of a low-pass filter, as such a filter is often used to remove noise unrelated to the evoked responses. Fig. 3 and Fig. 4 display the result of response onset time detection using different low-pass filter parameters for a SOBI component with auditory evoked responses. Filtering clearly removed more of the background noise and highlighted the signals associated evoked responses[1] (Fig. 3). There was no apparent change in the detected onset times and in the number of detections as the low-pass filter length changed from no filter to 40 Hz, 20 Hz and 10 Hz (Fig. 3) and as the roll off parameter was changed from 0.5 Hz to 5 Hz (Fig. 4). A quantitative comparison between the detected onset times using different low-pass filter length revealed very small changes in the number of onsets detected. When a more aggressive low-pass filter was used, the number of events detected was reduced from to 145 to 141 (out of a total of 150 trials).

If an onset time is only detectable when no filter is used, it is possible that such a detected response is a result of false detection due to noisy background ongoing activity. Therefore, by using a more aggressive low-pass filter, one can reduce the chance of false detection. On the other hand, a more aggressive filter can change the detected onset times. Thus, a change caused by low-filtering could be a result of better onset time estimation associated with a reduction in false detection or a result of temporal smearing due to filtering. To ensure that temporal smearing was not the cause of change in the detected onset times, we always performed the detection procedure

[1] Note that baseline fluctuations were larger than the false color would indicate.

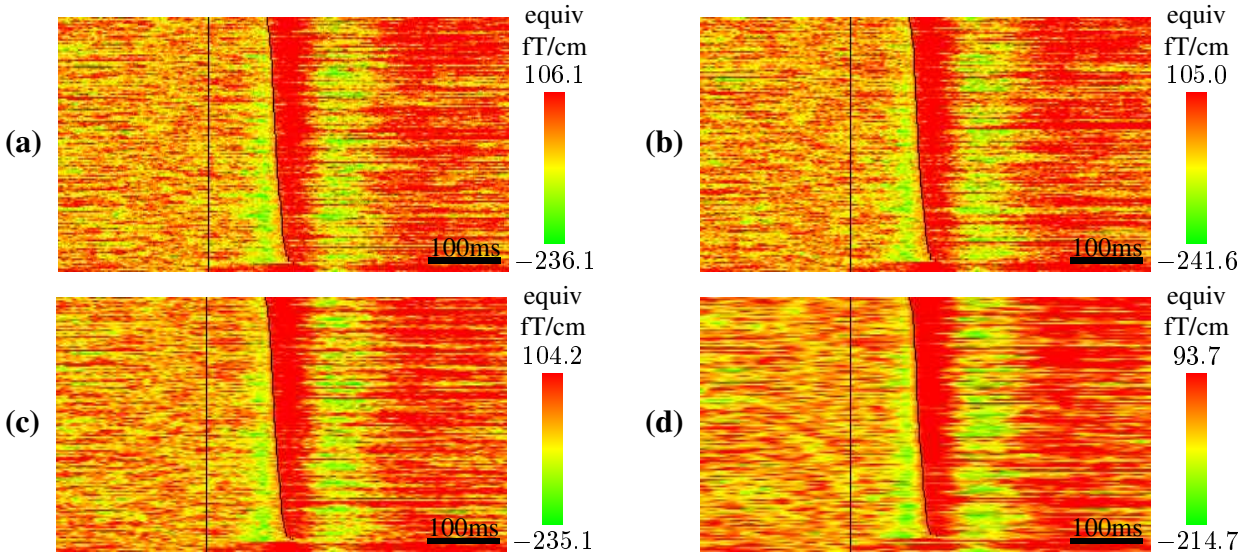

Figure 3: Effect of low-pass filter on response onset time detection (onset times, % response detected). **(a)** No filter: 90±1 ms; 96.7% **(b)** low-pass at 40 Hz: 91±1 ms; 96% **(c)** low-pass at 20 Hz: 92±1 ms; 95.3%. **(d)** low-pass at 10 Hz: 92±1 ms; 94%. For all panels, a roll-off of 5 Hz was used.

with and without filtering and examined graphically whether the filtering had introduced unwanted alteration in the temporal profile of the evoked response. In Fig. 3, filtering with a 10 Hz low-pass filter in this case only changed the estimated onset times by $<= 2$ ms and did not appear to distort the original evoked responses.

Because a more aggressive low-pass filter can remove the influence of background ongoing activity, thereby minimizing false detection, without significantly altering the temporal profile of the evoked responses, in the following analysis, a low-pass filter of 10 Hz with a roll off of 5 Hz was used unless otherwise specified. It is important to note that for different neuronal sources, the effect of a given filter on response onset times will be different. When a filter introduces significant change in the temporal profile of the evoked responses, a less aggressive filter length should be used for accurate estimation.

3.2 Response Onset Time Detection Across Sensory-Modality

In this section, we demonstrated that single-trial response onset time detection can be achieved in three major sensory modalities and under experimental conditions of both large and small trial-to-trial variability. Single-trial onset time detection with *large* trial-to-trial variability was performed for the visual and somatosensory evoked responses recorded during cognitive tasks described in Part I. Single-trial onset time detection with *smaller* trial-to-trial variability was performed for the auditory evoked responses recorded during a simple binaural pure tone presentation.

The detected response onset times are shown in MEG images (Fig. 5b), with the evoked responses aligned to the stimulus onset (time zero, marked by the vertical line on the left side of the MEG image) and the detected response times marked as a curve to the right of the stimulus onset line (DRT curve). The detection results are shown sorted according to the detected onset

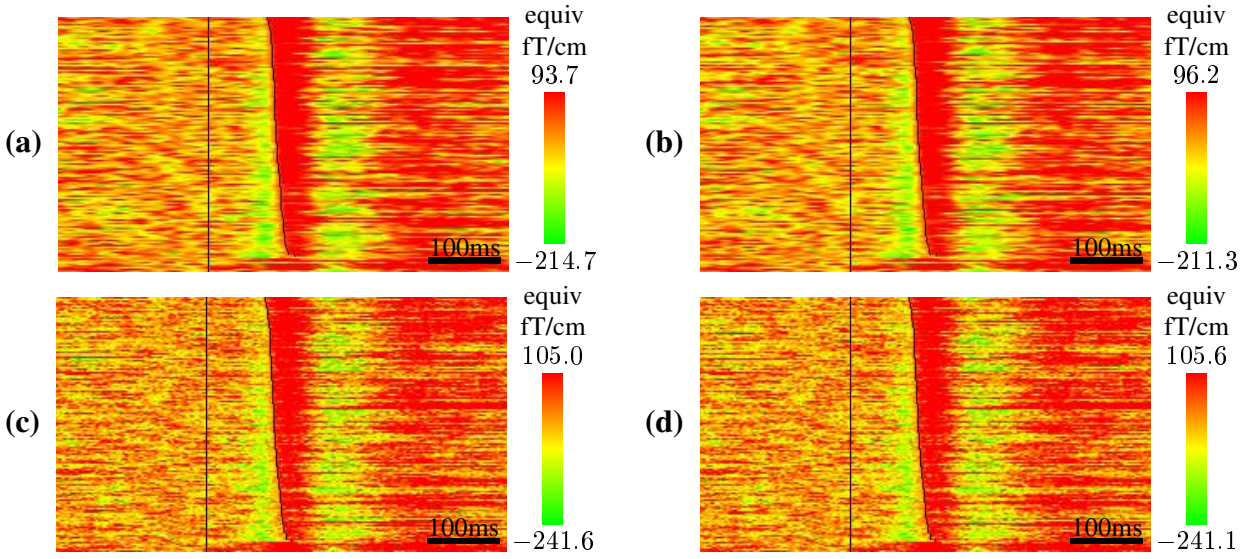

Figure 4: Effect of filter roll-off on response onset time detection (onset times, % response detected). **(a)** 10 Hz low-pass and 5 Hz roll-off: 92±1 ms, 94%. **(b)** 10 Hz low-pass and 0.5 Hz roll-off: 92±1 ms, 94%. **(c)** 40 Hz low-pass and 5 Hz roll-off: 91±1 ms, 96%. **(d)** 40 Hz low-pass and 0.5 Hz roll-off: 91±1 ms, 96%.

times. The stimulus-locked average (Fig. 5a), the sensor projections, or field maps (Fig. 5c), and the dipole location superimposed on the subject's MRI images (*e.g.* Fig. 5d) are also provided for comparison with results from standard analysis.

For the visual source shown in Fig. 5, the single-trial response onsets were detected in 64 of 90 trials (71.1%). The estimated onset times were 110.9±1.2 ms. The temporal profile in the average response, the field map, the contour plot, and the dipole location were characteristic of the typical visual sources from the occipito-parietal lobes.

For the somatosensory source shown in Fig. 6, the single-trial response onsets were detected in 129 of 150 trials (86%) when the contra-lateral thumb pressed the mouse button and in 105 of 120 trials (87.5%) when the ipsi-lateral thumb pressed the mouse button. The response onset times from the time when the button press was detected on the trigger line were −1.1±1.8 ms and 15.3±1.3 ms for the contra- and ispi-lateral activation respectively. These numbers indicate that the somatosensory responses could start as soon as the thumb movement was initiated; as soon as, or even before, the mouse button was completely depressed. The temporal profile in the average responses was slower in rising and broader in width in comparison to the typical responses evoked by median nerve stimulation. This was expected because somatosensory stimulation due to button press movement and feedback is much more prolonged and variable in comparison to stimulation by the brief and well-controlled median nerve shock stimulation. The field map, the contour plot, and the dipole location are consistent with activation of the hand region of the somatosensory cortex.

For the auditory source shown in Fig. 7, the single-trial response onsets were detected in out 141 of 150 trials (94%). The estimated response onset times were 91.6±.6 ms. The temporal profile in the average response, the field map, the contour plot, and the dipole location were characteristic of the typical auditory sources. This particular auditory SOBI component had a two-dipole solutions,

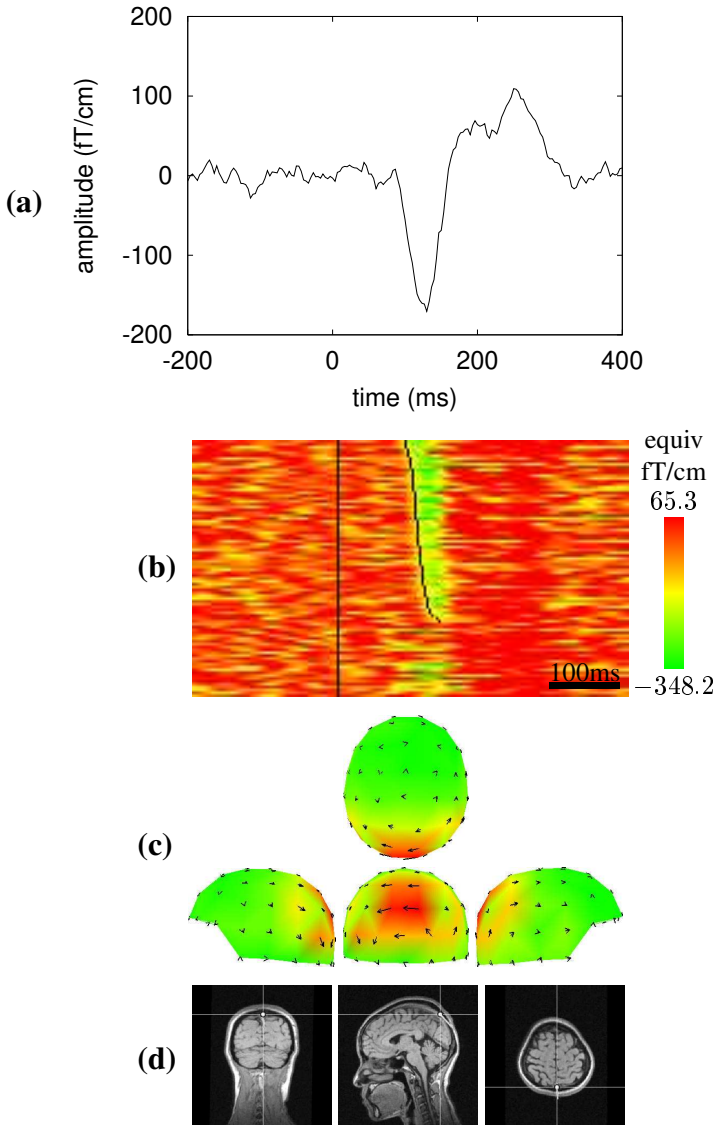

Figure 5: Detection of single-trial response onset times from a occipito-parietal source that responded to a visual stimulus. **(a)** Visual-stimulus-locked average response (unfiltered); **(b)** detected single-trial response times marked on an MEG image; **(c)** field map of the parietal source activation; **(d)** fitted ECD superimposed on the subject's MRI.

one in each of the two hemispheres, and both having the same time course of responses.

3.3 Visual response onset time detection cross-subject

As discussed in Part I, visual sources were identifiable along both the ventral and dorsal streams. The occipito-parietal sources along the dorsal stream varied less in location and in response profile. In contrast, the occipito-temporal sources along the ventral stream showed greater variability in response profile and precise location. To give the readers a sense of how well the single-trial onset

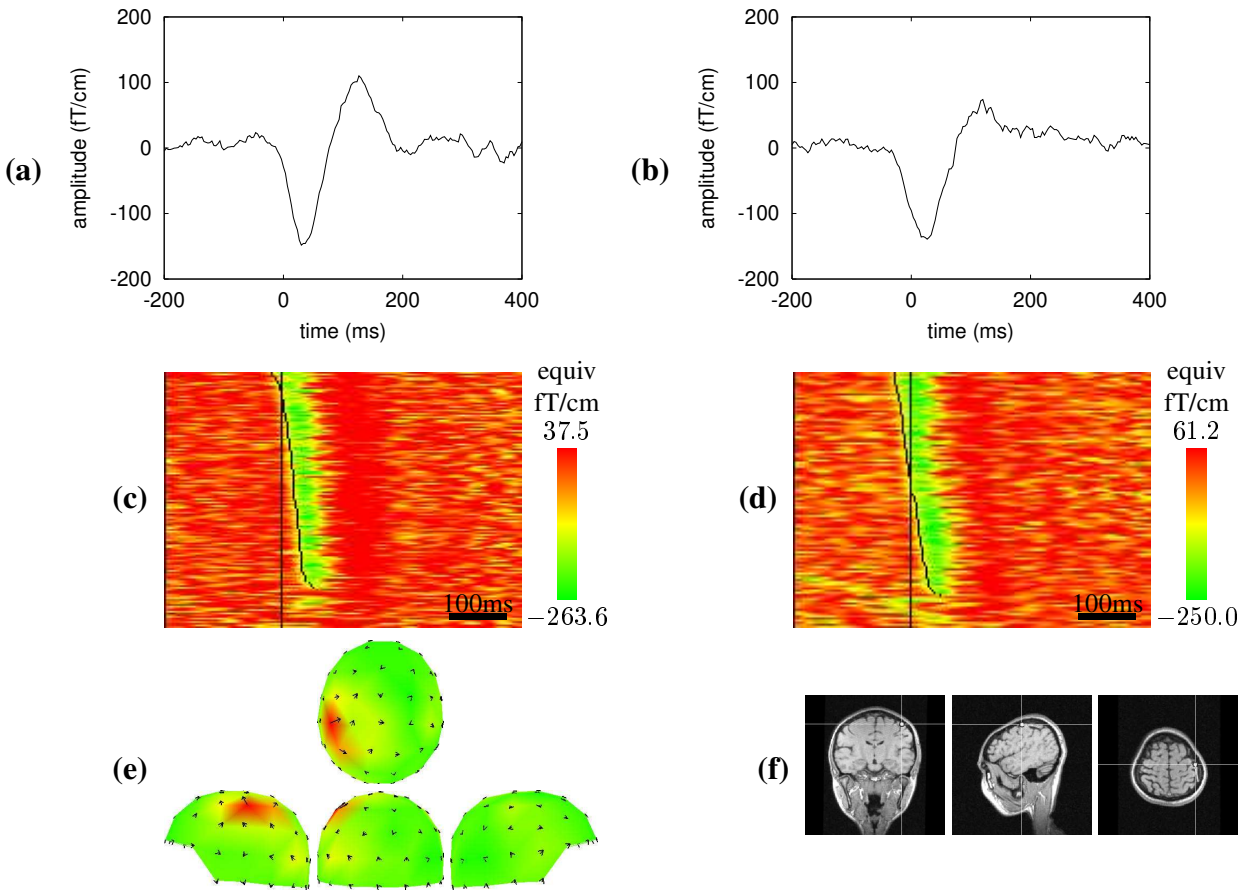

Figure 6: Detection of single-trial response onset times from a somatosensory (SS) source that responded to left **(a)** and right **(b)** button presses. **(ab)** Left and right button-press-locked average responses (unfiltered). **(c/d)** Detected single-trial response onset times triggered by left and right button presses respectively, marked on MEG images; **(e)** field map of the somatosensory source activation; **(f)** fitted ECD superimposed on the subject's MRI.

time detection procedure can perform across a variety of visual sources, we show detection for the most variable visual responses from multiple subjects.

In 13 of 16 (81%) expected visual sources along the ventral processing stream[2], single-trial onset time detection could be performed with a detection rate of 69.9±2.4%, and an estimated response onset times of 130.7±5.5 ms ($N = 13$). Fig. 8 shows results of onset time detection for the visual sources from each of the four subjects. Sources were chosen to reflect variability in the responses and in the detection.

[2]Given the tasks involved memory of visual forms, we expected at least one visual source to be activated along the ventral processing pathway. A total of 16 such sources are expected for 4 experiments in 4 subjects.

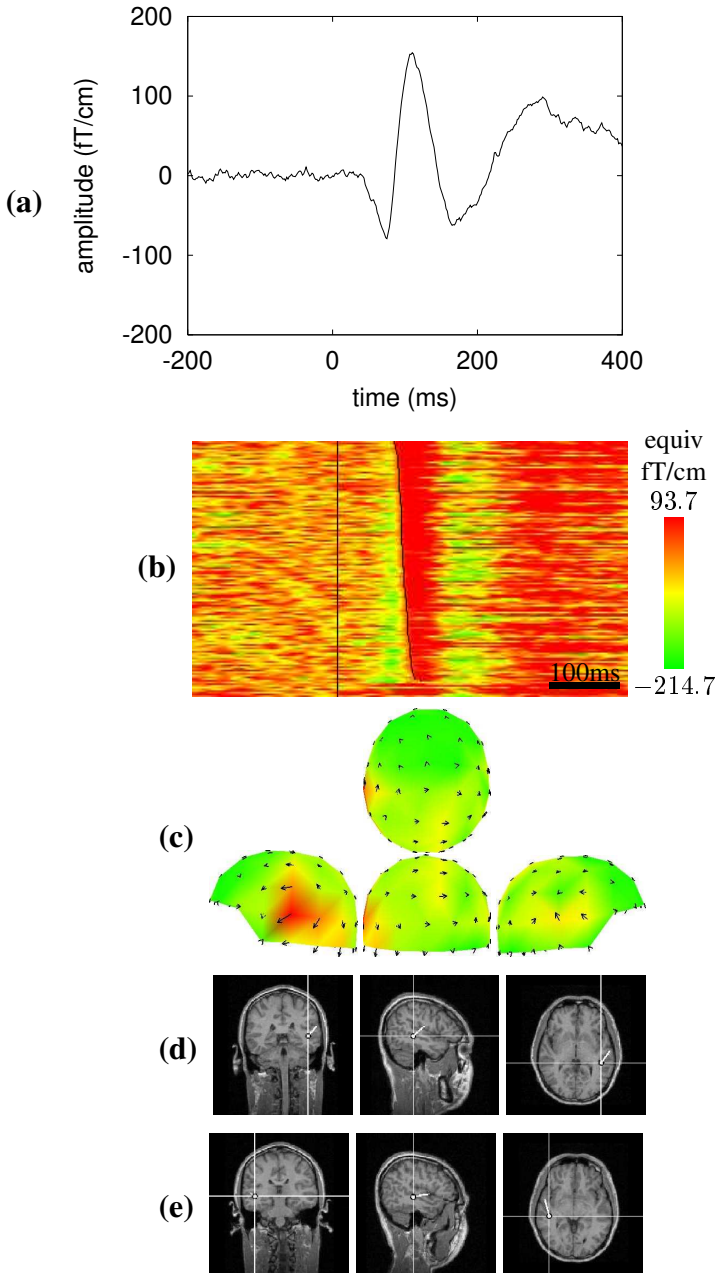

Figure 7: Detection of single-trial response onset times from an auditory source. **(a)** Auditory-stimulus-locked average response (unfiltered). **(b)** Detected single-trial response times marked on an MEG image. **(c)** Field map of the temporal source activation. **(d/e)** Fitted ECD superimposed on the subject's MRI.

3.4 Somatosensory response onset time detection cross-subject

As discussed in Part I, somatosensory sources can be identified in all subjects who made button press responses during the four cognitive tasks. Single-trial response onset time detection was attempted on one of the SOBI somatosensory components for each subject in at least one of the four

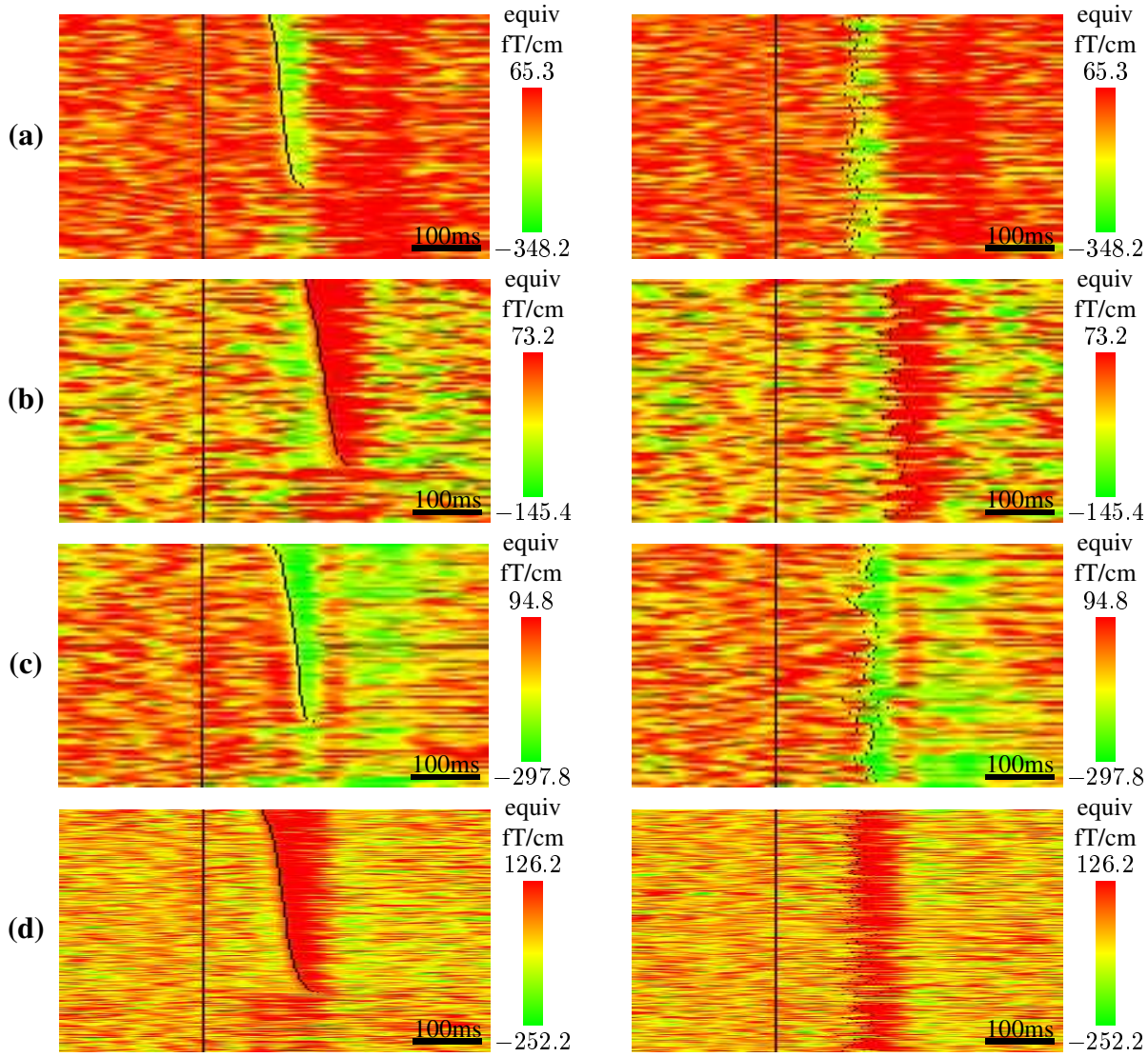

Figure 8: Single-trial visual response onset detection across multiple subjects, sorted by onset latency (left), and order of occurrence (right). **(a–d)** Subjects 1–4. For **(a–c)**, $N = 90$ trials. For **(d)**, $N = 270$ trials.

tasks. Because the activation of these somatosensory source were highly variable (see Part I), in only 7 of 24 somatosensory sources, single-trial onset time detection could be performed. Among these sources, for the contra-lateral button presses, single-trial onset times were estimated to be 0.0±2.5 ms with a detection rate of 81.0±2.4% ($N = 7$). For the ipsi-lateral button presses, single-trial onset times were estimated to be 4.5±2.6 ms with a detection rate of 75.6±5.4% ($N = 7$). Fig. 9 shows results of onset time detection for one such source in each of the three subjects.

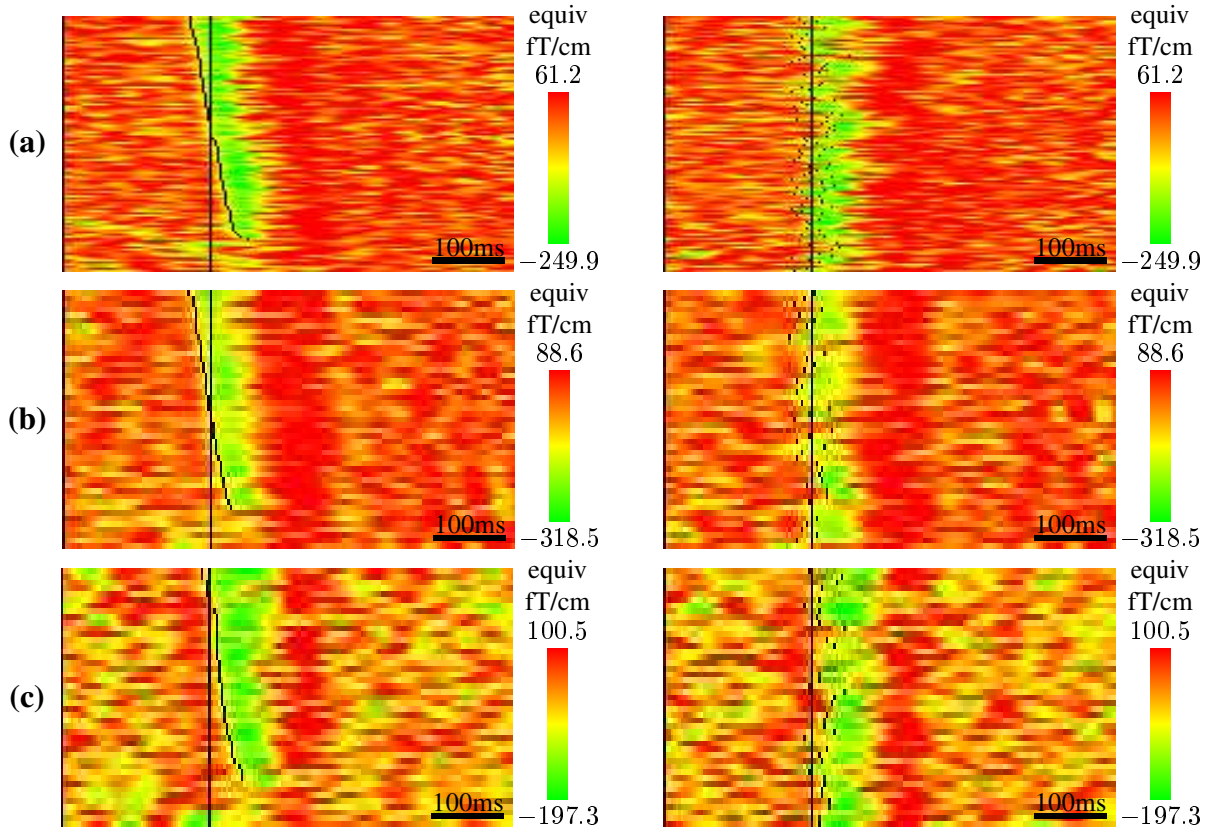

Figure 9: Single-trial somatosensory response onset detection across subjects, sorted by onset latency (left), and order of occurrence (right). **(a–c)** Subjects 1–3. Shown for contralateral activation only. The number of trials varied from subject to subject.

3.5 Auditory response onset time detection cross-subject

Auditory onset time detection was performed on data collected from six subjects during a simple auditory tone presentation. Auditory evoked responses from the presentation of a pure tone were the least variable in comparison to the above described visual and somatosensory responses from the cognitive tasks. In all six subjects, auditory sources can be identified and localized from the SOBI separated components. Single-trial response onset time detection could be performed in 6 of 6 expected auditory sources[3] with a detection rate of 80.3±2.7%, and estimated response onset times of 85.2±1.3 ms ($N = 6$).

Fig. 10 shows results of onset time detection for the auditory source from each subject. As the trial-to-trial variability auditory stimulation was very low in comparison to the variablity in the visual and somatosensory stimulation during the cognitive tasks, the average detection rate was higher for these auditory sources. Furthermore, single-trial response onset time detection could be performed among a higher percentage of subjects (100%) for the auditory responses than for the visual (81%) and somatosensory (29%) responses.

[3]Given the tasks involved auditory stimulation, we expected at least one auditory sources to be activated in each subject. A total of 6 auditory sources are therefore expected for the 6 subjects.

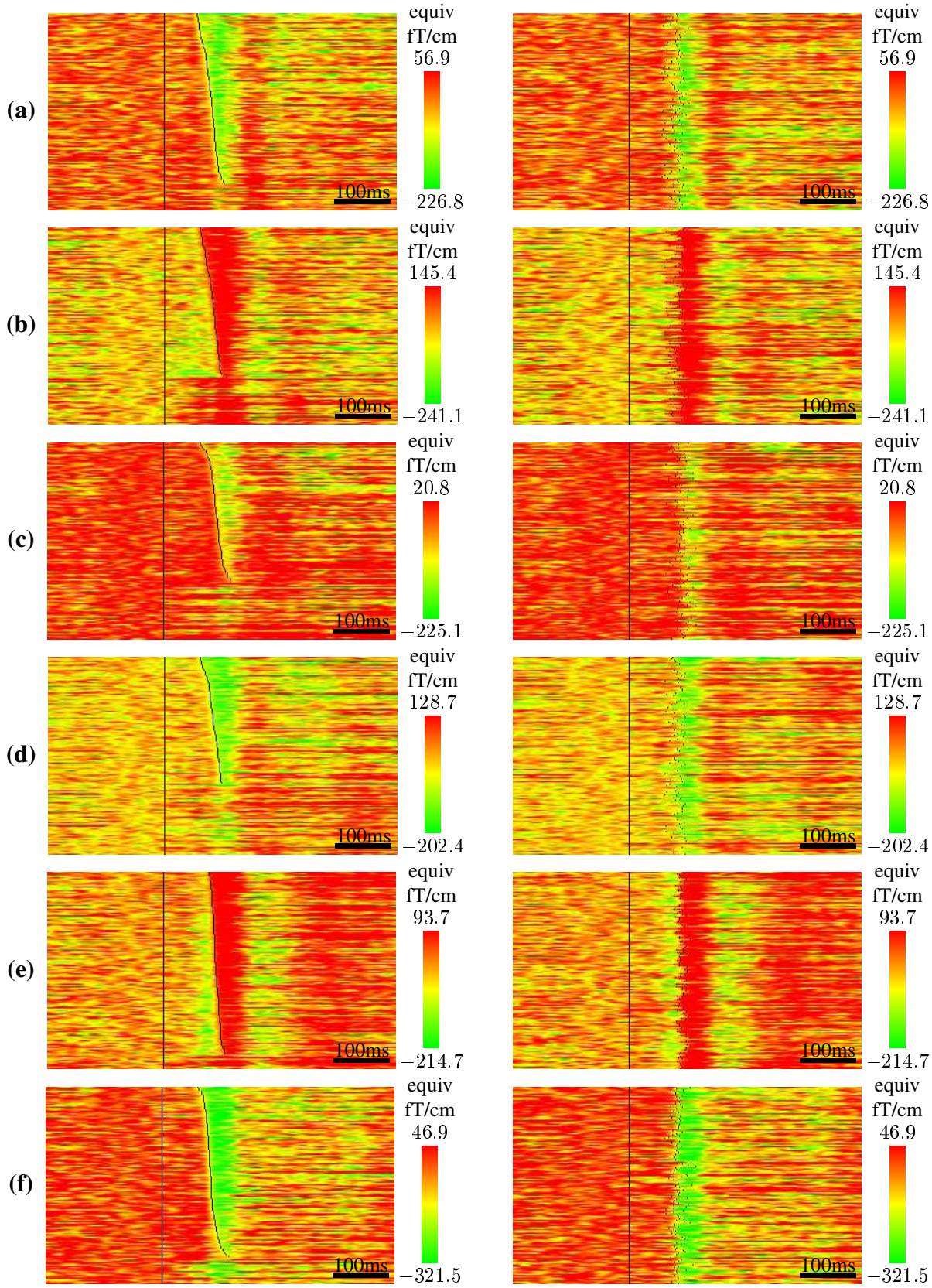

Figure 10: Single-trial auditory response onset detection across subjects, sorted by onset latency (left), and order of occurrence (right). **(a–f)** Subjects 1–6. $N = 150$ trials.

4 Discussion

By applying the SOBI algorithm to both noisy MEG data collected during cognitive tasks and cleaner MEG data from a simple sensory activation task , we were able to isolate neuronal sources in visual, auditory, and somatosensory modalities and to measure their single-trial response onset times with detection rates as high as 96%. These results show that, with the aid of ICA, it is possible to non-invasively measure single-trial response onset times in humans from specific neuronal populations with millisecond resolution. Such measurement can be obtained for multiple sensory modalities and can tolerate fairly large variability in both stimulus presentation and neuronal activation.

ICA-aided single-trial analysis was first applied to EEG data by Jung et al. (1999) using Bell and Sejnowski (1995) Infomax, another ICA algorithm. In this study, images of single-trial responses (ERP images) were shown for components separated by Bell-Sejnowski Infomax. The differences between that EEG result and our current results are (1) single-trial response onset times were not explicitly measured in the EEG study; (2) the ERP images of single-trial response were shown with vertical smearing via application of a filter across trials, and therefore do not reflect the true trial-to-trial variability; and (3) these EEG components were not localized to specific brain regions. More recently, Bell-Sejnowski Infomax has been used to analyze phase-shift in the ongoing rhythmic activity in EEG data (Makeig et al., 1999). With the introduction of high density EEG, improved spatial localization may be possible for EEG in the future.

In theory, single-trial response onset times could be obtained by employing dipole modeling method on the averaged data and then using the dipole source field patterns. In practice, single-trial response onset time estimation using such a method was not routinely performed in MEG studies. ICA methods, along with the magnetic field tomography method (MFT) (Ioannides et al., 1995; Liu and Ioannides, 1996; Liu et al., 1999; Ioannides et al., 2000), are the few methods explicitly offering the promise of single-trial response onset time measurement. SOBI differs from MFT in that the separation of a neuronal source from noise sources and from other neuronal sources is based on the temporal information alone. Therefore SOBI does not suffer from two types of potential errors: (1) numeric errors in the forward model and (2) errors arising from assumptions made in the spatial domain, such as how distributed a neuromagnetic source is. Using SOBI, separation and identification of neuronal sources is not limited by whether the neuronal populations activated is a point or distributed source. One can measure response onset times of discontiguous neuronal populations, as long as they show coherent activation. SOBI, and ICA methods in general, also differ from MFT in that they can take advantage of other source localization methods by serving as a front end. Single or multiple dipole methods and point or distributed source analysis methods can all be used on SOBI's output.

To fully benefit from the capability of measuring single-trial response onset, it is critical that the response onset be detected in a reasonable proportion of the trials. Therefore, it is important to point out that the proportion of the trials in which the response onset times can be estimated depends on a number of factors. Low detection rates can result from poor separation, which gives rise to residual sensor and environmental noise in the separated neuronal components. It can also result from poor execution of the detection procedure. Most importantly, a low detection rate can be a direct consequence of non-methodological factors, including a high amplitude of baseline neuronal signal fluctuation, a high amplitude of baseline neuronal oscillatory activity, a

high variability in the stimulus presentation, or a high variability in the neuronal source activation due to the specific behavioral task. As shown by this study, whether single-trial response onset times could be measured for a given source depends on the variability in the sensory stimulation involved. The smaller the variability in the sensory stimulation (*e.g.* as in the auditory stimulation), the more likely single-trial response onset times could be obtained for a given neuronal source. Therefore, a low detection rate is not necessarily indicative of poor performance in separation and detection *per se*. To improve the detection rate, one should always strive for a careful experimental design that minimizes unnecessary trial-to-trial variability.

Our demonstrated capability in single-trial measurement of response onset times from a spatially localizable neuronal population can have a significant impact on the field of cognitive neuroscience. In the area of sensory processing, relative timing of neuronal activation in different neuronal populations during sensory stimulation can be critical in determining the coherence of the percept (Bartels and Zeki, 1998). In perceptual learning, a single experience can change the perception of an otherwise initially ambiguous stimulus. We expect that non-invasive single-trial response onset time measurement in humans will enable the investigation of neural correlates of a wide range of time-sensitive perceptual and learning phenomena.

Acknowledgements

Supported by the National Foundation for Functional Brain Imaging and NSF CAREER award (97-02-311), an equipment grant from Intel corporation, the Albuquerque High Performance Computing Center, a gift from George Cowan, and a gift from the NEC Research Institute. We thank researchers from the Helsinki group for helping with packaging the BSS components for the Neuromag software. We are indebted to Mike Weisend who granted us access to his data and to Robert Christner for technical support.

References

Abeles, M., Bergman, H., Margalit, E., and Vaadia, E. (1993). Spatiotemporal firing patterns in the frontal cortex of behaving monkeys. *J. Neurophysiol.*, 70:1629–1638.

Bartels, A. and Zeki, S. (1998). The theory of multistage integration in the visual brain. *Philos. T. Roy. Soc. B.*, 265(1412):2327–2332.

Bell, A. J. and Sejnowski, T. J. (1995). An information-maximization approach to blind separation and blind deconvolution. *Neural Computation*, 7(6):1129–1159.

Belouchrani, A., Meraim, K. A., Cardoso, J.-F., and Moulines, E. (1993). Second-order blind separation of correlated sources. In *Proc. Int. Conf. on Digital Sig. Proc.*, pages 346–351, Cyprus.

Cao, J. T., Murata, N., Amari, S., Cichocki, A., Takeda, T., Endo, H., and Harada, N. (2000). Single-trial magnetoencephalographic data decomposition and localization based on independent component analysis approach. *IEICE Transactions on Fundamentals of Electronics, Communications and Computer Sciences*, E83A(9):1757–1766.

Cardoso, J.-F. (1994). On the performance of orthogonal source separation algorithms. In *European Signal Processing Conference*, pages 776–779, Edinburgh.

deCharms, R. C. and Merzenich, M. M. (1996). Primary cortical representation of sounds by the coordination of action-potential timing. *Nature*, 381:610–613.

Huerta, P. T. and Lisman, J. E. (1993). Heightened synaptic plasticity of hippocampal CA1 neurons during a cholinergically induced rhythmic state. *Nature*, 364:723–725.

Ioannides, A. A., Liu, L. C., Theofilou, D., Dammers, J., Burne, T., Ambler, T., and Rose, S. (2000). Real time processing of affective and cognitive stimuli in the human brain extracted from MEG signals. *Brain Topogr.*, 13(1):11–19.

Ioannides, A. A., Liu, M. J., Liu, L. C., Bamidis, P. D., Hellstrand, E., and Stephan, K. M. (1995). Magnetic-field tomography of cortical and deep processes: examples of real-time mapping of averaged and single trial MEG signals. *Inter. J. of Psychophysiol.*, 20(3):161–175.

Jung, T.-P., Makeig, S., Westerfield, M., Townsend, J., Courchesne, E., and Sejnowski, T. J. (1999). Analyzing and visualizing single-trial event-related potentials. In *Advances in Neural Information Processing Systems 11*, pages 118–124. MIT Press.

Liu, B. C., Ioannides, A. A., and Streit, M. (1999). Single trial analysis of neurophysiological correlates of the recognition of complex objects and facial expressions of emotion. *Brain Topogr.*, 11(4):291–303.

Liu, L. C. and Ioannides, A. A. (1996). A correlation study of averaged and single trial MEG signals: the average describes multiple histories each in a different set of single trials. *Brain topography*, 8(4):385–396.

Makeig, S., Townsend, J., Jung, T.-P., Enghoff, S., Gibson, C., Sejnwoski, T. J., and Courchesne, E. (1999). Early visual evoked response peaks apper to be sums of activity in multiple alpha sources. *Soc. Neurosci. Abstr.*, 25(652.8).

Markram, H., Lubke, J., Frotscher, M., and Sakmann, B. (1997). Regulation of synaptic efficacy by coincidence of postsynaptic aps and epsps. *Science*, 275:213–5.

Rieke, F., Warland, D., de Ruyter van Steveninck, R., and Bialek, W. (1996). *Spikes: Exploring the Neural Code*. MIT Press.

Sejnowski, T. J. (1995). Time for a new neural code? *Nature*, 376:21.

Tang, A. C., Pearlmutter, B. A., and Zibulevsky, M. (1999). Blind separation of multichannel neuromagnetic responses. In *Computational Neuroscience*, pages 1115–1120. Published in a special issue of *Neurocomputing* volume 32–33 (2000).

Tang, A. C., Pearlmutter, B. A., Zibulevsky, M., Hely, T. A., and Weisend, M. P. (2000). An MEG study of response latency and variability in the human visual system during a visual-motor integration task. In *Advances in Neural Information Processing Systems 12*, pages 185–191. MIT Press.

Vigário, R., Jousmäki, V., Hämäläinen, M., Hari, R., and Oja, E. (1998). Independent component analysis for identification of artifacts in magnetoencephalographic recordings. In *Advances in Neural Information Processing Systems 10*. MIT Press.

Vigário, R., Sarela, J., Jousmaki, V., and Oja, E. (1999). Independent component analysis in decomposition of auditory and somatosensory evoked fields. In *Proc. First International Conference on Independent Component Analysis and Blind Source Separation ICA'99*, pages 167–172, Aussois, France.

Wilson, M. A. and McNaughton, B. L. (1994). Reactivation of hippocampal ensemble memories during sleep. *Science*, 265(5172):676–679.